One-Dimensional Nanostructures for Photodetectors

Guozhen Shen* and Di Chen

Wuhan National Laboratory for Optoelectronics and College of Optoelectronic Science and Engineering, Huazhong University of Science and Technology, Wuhan 430074, P. R. China

Received: November 2, 2009; Accepted: November 10, 2009; Revised: November 17, 2009

Abstract: With large surface-to-volume ratios and Debye length comparable to their small size, one-dimensional nanostructures have been extensively studied and have been widely used to fabricate many high-performance and new type nanoscale electronic and optoelectronic devices. In this work, we provide a comprehensive review on the state-to-the-art research activities on the photodetectors application of one-dimensional nanostructures. The review begins with a survey of the patents and reports on the synthesis of one-dimensional nanostructures, which can be used to fabricate photodetectors. Then the recent progress on this topic is discussed, focusing on 1-D metal oxide, III-V group semiconductors, and other nanomaterials. This review will then be finalized with some perspectives and outlook on the future developments of this research topic.

Keywords: Nanowires, photodetectors, one-dimensional nanostructures, field-effect transistors.

INTRODUCTION

One-dimensional (1-D) nanostructures are the focus of recent research efforts in nanotechnology due to their special shapes, compositions, doping states, chemical and physical properties [1-42]. Nowadays, 1-D nanostructures can be rationally synthesized in single crystal form with all key parameters controllable, such as chemical composition, shapes, doping state, diameter, length, etc. [1-42]. They represent the smallest dimension structure that can efficiently transport electrical carriers and thus are ideally suited to fabricate nanoscale electronics and optoelectronics. With large surface-to-volume ratios and Debye length comparable to their small size, the electronic property of 1-D nanostructures is strongly influenced by the surface processes, thus yields superior sensitivity than their thin film counterpart [5-8].

Configured as either nanoscale field-effect transistors (FETs) or resistors, 1-D nanostructures can be used to fabricate high-performance photodetectors. The sensing mechanism of 1-D nanostructure photodetectors has been investigated recently [43,44]. We give here a brief description about the sensing mechanism by using zinc oxide nanowires as a model system [44]. Figure **1a** is a schematic of a nanowire photodetector. Briefly, electron-hole pairs are photogenerated once the nanowire is illuminated with photon energy larger than the nanowire band gap. The holes can be easily trapped at the surface, leaving behind unpaired electrons, which results in the increase of the conductivity under an applied electric field. Figure **1b** and **1c** display the schematics of the nanowire energy band diagrams in dark and under illumination, respectively. As illustrated here, in the dark, oxygen molecules absorbed on the nanowire surface capture free electrons via $O_2(g) + e^- \rightarrow O_2^-(ad)$, and a low-conductivity depletion layer is formed near the surface. Once illuminated with light at a photon energy above the energy gap, electron-hole pairs are photogenerated via $h\nu \rightarrow e^- + h^+$, and the holes migrate to the surface, resulted in the photodesorption of oxygen from the nanowire surface [$h^+ + O_2^-(ad) \rightarrow O_2(g)$]. It is thought that thinner nanowires lead to lower photoresponses, while thicker nanowires will not imply any further signal enhancement. Thus it is very important to choose nanowires with suitable diameters.

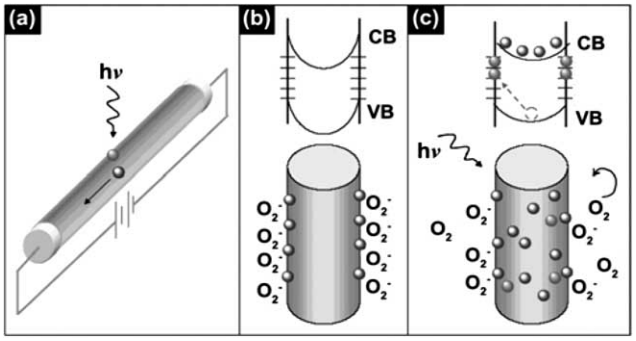

Fig. (1). (**a**) Schematic of a nanowire photodetector. (**b,c**) the energy band diagrams of a nanowire in dark and upon illumination. Reproduced with permission from *Nano Lett.* **2007**, *7*, 1003. Copyright **2007** *American Chemical Society*.

Compared with bulk and thin film materials, the enhanced sensitivity of 1-D nanostructures to light irradiation is usually interpreted as a result of large surface-to-volume ratio. Here, we intend to provide an overview on this interesting photodetecting field. First, synthetic methods developed to get typical 1-D nanostructures that can be used to fabricate photodetectors are surveyed. The patents and reports on photodetectors built on 1-D nanostructures will

* Address correspondence to this author at Wuhan National Laboratory for Optoelectronics and College of Optoelectronic Science and Engineering, Huazhong University of Science and Technology, Wuhan 430074, P. R. China; Fax: 86-27-87792223; E-mails: gzshen@mail.hust.edu.cn; gzshen@ustc.edu

1872-2105/10 $100.00+.00

then be introduced. Finally, we conclude the review with some perspectives and outlook.

SYNTHESIS OF 1-D NANOSTRUCTURES

Bottom-up method is one of the most important methods developed to synthesize 1-D nanostructures because it provides a reliable method to get single-crystalline, high optical quality materials. With this method, 1-D nanostructures can be rationally synthesized in single crystal form with controlled key parameters during growth, such as chemical composition, doping state, diameter, length, etc. [45-60]. Till now, 1-D nanostructures, such as nanowires, nanotubes, nanorods, nanobelts, nanorings, and hetero-nanowires, can be produced for a host of materials, including metal oxides, III-V and II-VI group semiconductors, metals, polymers, by using techniques like solution methods, template-assisted methods, vapor-phase methods, electrospinning, and so on. In this section, we will briefly introduce some typical 1-D nanostructures synthesized from different methods that are suitable to fabricate nanoscale photodetectors [45-93].

Table **1** lists the state-of-the-art progress of different 1-D nanostructures synthesized from different methods that are used to fabricate nanoscale photodetectors [45-93]. Figure **2a** shows a scanning electron microscopy (SEM) image of CdS nanoribbons synthesized from a thermal chemical vapor deposition method [80]. During this process, CdS powder was used as the source material and Au-coated silicon substrates were used to collect the deposited product. From the SEM image, it can be seen that the surface of the produced nanoribbons are clean and smooth. The width and thickness are in the range of 2-40 μm and 10-60 nm, respectively. The microstructure of the synthesized CdS nanoribbons were studied by high-resolution transmission electron microscopy (HRTEM) and the image is shown in Fig. (**2b**). The marked lattice fringe is 0.335 nm, corresponding to the [002] plane of hexagonal CdS phase. A selected area electron diffraction (SAED) pattern taken from the nanoribbon is shown in Fig. (**2b**) inset. Combined the SAED and HRTEM results, it was deduced that the CdS nanoribbons are hexagonal single crystals with the preferred growth directions along the [112] orientation. Using the chemical vapor deposition method, many other binary 1-D nanostructures, including CdSe, ZnS, GaN, InP, SnO_2, ZnO, In_2O_3, Ga_2O_3, etc. are also produced under controlled experimental conditions.

Solution methods provide another group of methods that are able to produce high quality 1-D nanostructures for photodetectors. Figure **3** is the results on Se nanowires, which were synthesized through a "solid-solution-solid" growth process by dispersing Se spheres in ethanol [94]. The Se spheres precursors were prepared by dismutation of Na_2SeSO_3 solution at room temperature. Figure **3a** is the SEM image of the obtained Se nanowires, which have diameters of ~160 nm and lengths of up to several tens of micrometers. A TEM image of a single Se nanowire is illustrated in Fig. (**3b**), indicating smooth and clear surface. Figure **3c** is a HRTEM image taken from the Se nanowire. The clearly resolved fringe spacing is 0.5 nm, in agreement with the (001) planes of trigonal Se phase. The inset of Fig.

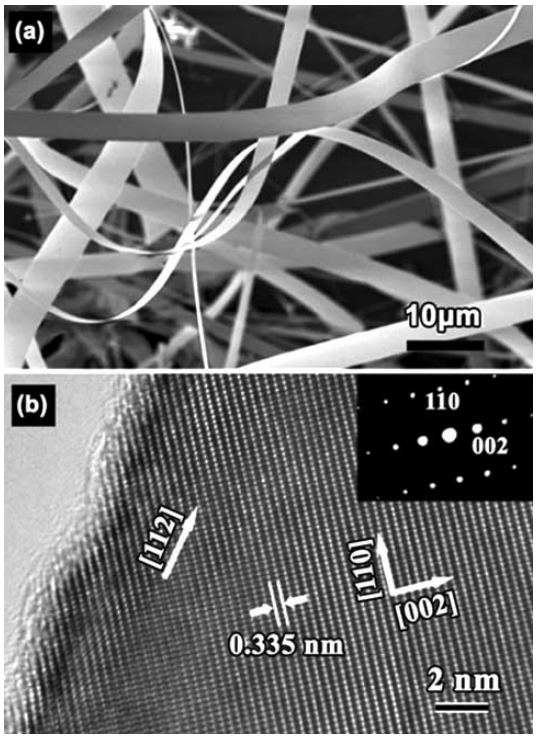

Fig. (2). (**a**) SEM image and (**b**) HRTEM image of CdS nanoribbons. Reproduced with permission from *Nano Lett.* **2006**, *6*, 1887. Copyright **2006** *American Chemical Society*.

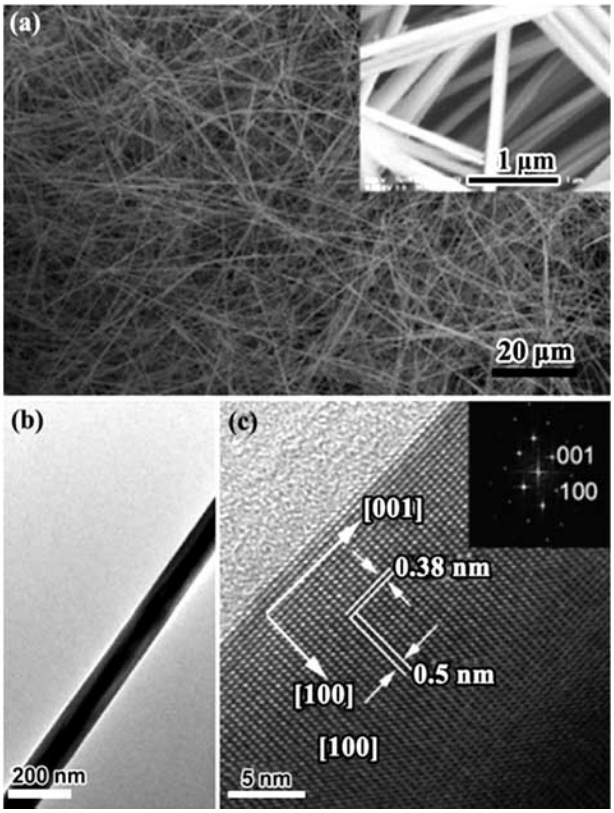

Fig. (3). (**a**) SEM image, (**b**) TEM image and (**c**) HRTEM image of Se nanowires produced by a sonication process. Reproduced with permission from *Nano Res.* **2008**, *1*, 403. Copyright **2008** *Tsinghua Press and Springer-Verlag*.

Table 1.

Materials	Morphology	Synthetic Method	Dark Current/Conductance	Photocurrent/Conductance	Ref.
ZnO	Ultralong nanowires	chemical vapor deposition method	>10 GΩ	1-5 orders of magnitude lower in resistance	[45]
	nanowires	Vapor phase transport process	3.5 MΩcm	4-6 orders of magnitude lower in resistance	[46]
	nanowires	Chemical vapor deposition method	1-10 nA	100 μA	[44]
	Vertically aligned nanowires	Thermal evaporation method	/	/	[47]
	nanorods	Hydrothermal method	0.20 Ωcm		[48]
	nanowires	Metal organic chemical vapor deposition	~110μA	~170μA	[49]
	nanowires	Pulsed-laser deposition	/	/	[50]
	Ag-ZnO Heterostructured nanowires	Electrospinning process	1800 times increase in photocurrent	/	[51]
	Nanowire film	Sol-gel method	4.32×10^{-9} A	5.11×10^{-7} A	[52]
	Vertically-aligned nanoneedles	Metal organic chemical vapor deposition	/	/	[53]
	nanowires	Thermal evaporation method	/	/	[54]
	Vertically aligned nanowires	Thermal evaporation method	1.35×10^{-5} A	2×10^{-7} A	[55]
	tetrapod	Solution method	/	/	[56]
SnO_2	nanowires	Thermal chemical vapor deposition method	0.12 μS	83.9μS	[57]
	Nanowires decorated with Au nanoparticles	Thermal chemical vapor deposition method	/	/	[58]
	nanowires	Thermal chemical vapor deposition method	7.7×10^{-5} A	1.3×10^{-4} A	[59]
	nanowires	Laser-assisted chemical vapor deposition method	0.66 nS	760 nS	[60]
In_2O_3	nanowires	Laser-assisted chemical vapor deposition method	/	290 nA	[61]
CdO	nanoneedles	Thermal chemical vapor deposition method	13.3 nS	114.5 nS	[62]
Ga_2O_3	nanowires	Thermal chemical vapor deposition method	15 pA	10 nA	[63]
Cu_2O	nanowires	Thermal oxidation	0.7 nS	4.3 nS	[64]
CeO_2	nanowires	Wet chemical route	22.8 nA	0.25 nA	[65]
Fe_2O_3	nanobelts	Thermal oxidation	10 nA	123 nA	[66]
MoO_3	nanobelt	Solution method	/	/	[67]
$ZnGa_2O_4$	nanowires	Thermal evaporation	8.5 pA	1 nA	[68]
$ZnSnO_3$	nanowires	Thermal evaporation	0.3 nA	162 nA	[69]

(Table 1) Contd….

Materials	Morphology	Synthetic Method	Dark Current/Conductance	Photocurrent/Conductance	Ref.
WO_3	nanowires	Thermal evaporation	/	/	[70]
GaN	nanowires	Thermal chemical vapor deposition method	/	/	[71]
	nanowires	Thermal chemical vapor deposition method	1.3 nS	23.4 nS	[72]
	nanofibers	electrospinning	/	830 time increased in conductance	[73]
	nanowires	Thermal chemical vapor deposition method	/	/	[74]
GaAs	nanowires	Catalytic chemical vapor deposition method	/	/	[75]
InP	nanowires	Laser-assisted catalytic growth	/	/	[76]
Si_3N_4	nanowires	Combustion synthesis	/	/	[77]
CdS	nanobelts	Thermal evaporation	/	Four orders of magnitude higher in conductance	[78]
	nanobelts	Thermal evaporation	80 pA	100 μA	[79]
	nanoribbons	chemical vapor deposition method	0.21 nS	128 nS	[80]
CdSe	nanoribbons	Thermal evaporation method	2pS	19 nS	[81]
	nanoribbons	Thermal chemical vapor deposition method	0.095 nS	1734 nS	[82]
ZnTe	nanowires	Hydrogen assisted thermal evaporation	3.08 nS	4.21 nS	[83]
InSe	nanowires	Physical vapor transport	40 pA	2000 pA	[84]
ZnSe	nanobelt	Solvothermal-thermal annealing method	Below 10^{-14} A	1.7 pA	[85]
Si	p-i-n nanowires	Catalytic chemical vapor deposition method	/	/	[86]
	nanowires	Chemical vapor deposition method	/	/	[87]
Se	nanowires	Solution method	/	100 times higher	[88]
Ge	nanowires	Chemical vapor deposition method	/	/	[89]
RuO_2/TiO_2	core/shell nanowires	Chemical vapor deposition method	18.5 μA	19.4 μA	[90]
$ZnSe/SiO_2$	Core/shell nanocables	Chemical vapor deposition method	70.5 pS	123 pS	[91]
ZnS-decorated InP	Hierarchical heteronanowires	Thermal chemical vapor deposition method	/	/	[92]
InAsP/InP	Core/shell nanowires	Chemical beam epitaxy	70 nS	813 nS	[93]

(**3c**) is a fast Fourier transform of the HRTEM image. The results indicate that the synthesized Se nanowires are single crystals with growth direction along the [001] plane.

Electrospinning process as a new method has been used to fabricate many materials. In this process, a polymer solution of melt is exposed to an electric field and at a critical voltage, the electric field will overcome the surface tension of the polymer and a jet will be extruded. Electrospinning method was used to fabricate 1-D nanostructures recently. For example, Fig. (**4**) shows the SEM images and TEM images of electrospinning synthesized GaN nanofibers [73]. The synthetic process includes three steps: 1) the

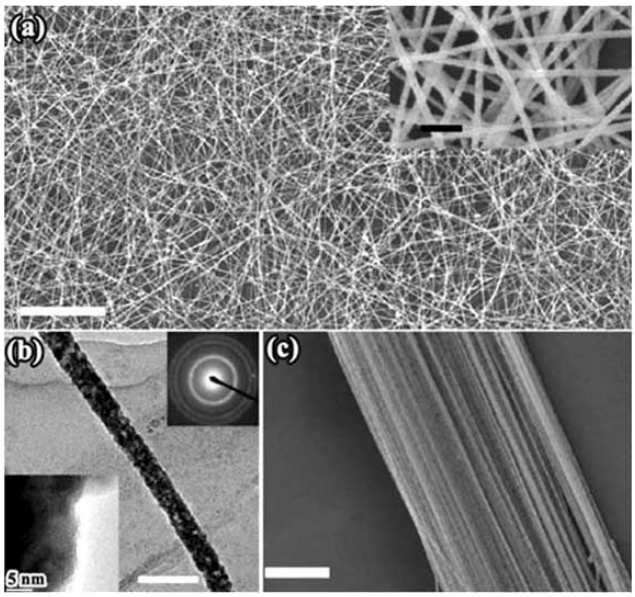

Fig. (4). (**a**) SEM image, (**b**) TEM image of GaN nanofibers. (**c**) SEM image of a bundle of oriented GaN nanofibers. Scale bars: (**a**) 5 μm, (**b**) 100 nm, (**c**) 1 μm. Reproduced with permission from *Adv. Mater.* **2009**, *21*, 227. Copyright **2009** *Wiley-VCH*.

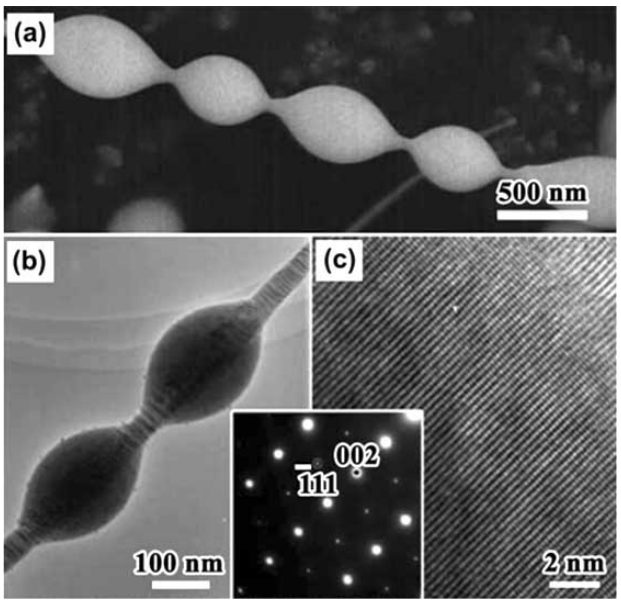

Fig. (5). (**a**) SEM image, (**b**) TEM image and (**c**) HRTEM image of pearl-like ZnS-decorated InP nanowire heterostructures. Reproduced with permission from Chem *Mater.* **2008**, *20*, 6779. Copyright **2008** *American Chemical Society*.

electrospinning of a composite nanofibers composed of gallium nitrate and polymer, 2) the calcination of the composite nanofibers to form gallium oxide nanofibers, 3) conversion gallium oxide nanofibers to gallium nitride nanofibers. After synthesis, GaN nanofibers with uniform diameters and lengths were obtained on a large scale. TEM image and the SAED pattern in Fig. (**4b**) reveal that the nanofibers are polycrystalline with the crystalline size of less than 10 nm. Using this technique, aligned GaN nanofibers were also able to be produced as shown in Fig. (**4c**).

With modulated compositions, structures, interface, and doping states, 1-D hetero-nanostructures have recently become of particular interest with respect to their potential applications in electronics and optoelectronics. Figure **5a** shows the SEM image of interesting pearl-like ZnS-decorated InP nanowire heterostructures synthesized from a chemical vapor deposition method [92]. The diameter of the trunk part of the heterostructures is smaller than 50 nm and the maximum diameters for the bulb parts are in the range of 100-400 nm. A TEM image of the heterostructures was shown in Fig. (**5b**), which also confirms the pearl-like structure. Figure **5c** is a HRTEM image taken from the trunk part. The resolved interplannar d-spacings perpen-dicular and parallel to the nanowire are 0.34 and 0.21 nm respectively. They correspond to the [111] and [220] planes of cubic InP phase, respectively. The results suggests that the trunk InP nanowires are single crystals with preferred growth direction along the <111> orientation and the bulb ZnS are polycrystalline.

PHOTODETECTORS BUILT ON DIFFERENT 1-D NANOSTRUCTURES

1-D Metal Oxide Nanostructures as Photodetectors

1-D metal oxide nanostructures are the focus of current research efforts since they are the commonest minerals in the earth. 1-D metal oxide nanostructures have been extensively investigated to fabricate nanoscale photodetectors. The valuable materials include binary metal oxides like ZnO, SnO_2, In_2O_3, CdO, Ga_2O_3, Cu_2O, CeO2, Fe_2O_3, WO_3, MoO_3, and ternary metal oxide like $ZnSnO_3$, $ZnGa_2O_4$.

With a wide band gap of 3.37 eV at room temperature and a large exciton binding energy of 60 meV, 1-D ZnO nanostructures have been widely used to fabricate nanoscale photodetectors. Yang *et al*. reported and patented the first ZnO nanowire photodetectors in 2002 [46]. The nanowires used were synthesized from a vapor transport process. After synthesis, electron beam lithography was used to fabricate gold electrodes on top of the ZnO nanowires. A SEM shown in Fig. (**6a**) inset shows the structure of the single nanowire photodetector. Figure **6a** shows the I-V curves of the device measured in dark and upon UV-light exposure,

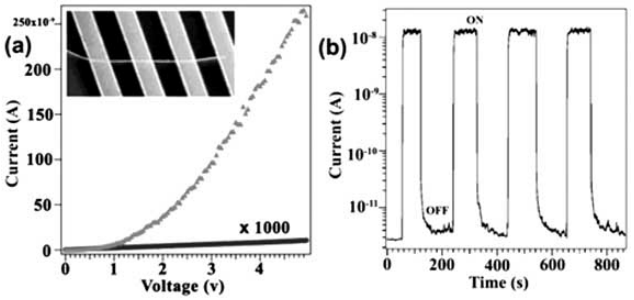

Fig. (6). (**a**) I-V curves show dark current and photocurrent of a single ZnO nanowire under 365 nm, 0.3 mWcm-2 UV-light illumination. (**b**) Reversible switching of a ZnO nanowire between low and high conductivity states when the UV-lamp was turned on and off. Reproduced with permission from *Adv. Mater.* **2002,** *14*, 158. Copyright **2002** *Wiley-VCH*.

respectively. From these curves, it can be seen that the nanowire is highly insulating in the dark with a resistivity above 3.5 MΩcm, while the resistivity decreased by typically 4 to 6 orders of magnitude when it was exposed to UV-light with wavelengths below 380 nm. The dramatic change of conductance between dark and UV exposure suggest that the ZnO nanowire photodetectors are good candidates for optoelectronic switches, with the dark state as "OFF" and the UV exposed state as "ON" and the result was shown in Fig. (**6b**). It is evident that the nanowire photodetectors can be reversibly switched between the low and the high conductivity state with rise and decay times below the detection limit.

Inspired by this work, many kinds of photodetectors have been fabricated by using different 1-D ZnO nanostructures [43-45, 47-56]. Table **1** gives a brief summary of the representative results on photoconducting behaviors of different 1-D ZnO nanostructures. It should be mentioned that, till now, the lack of well-established fabrication methods and standard procedures make it difficult to compare the experimental results between different devices, though some pioneer work has been done recently [43].

Tin oxide (SnO_2) is an important n-type semiconducting with very good sensitivities, including chemical sensing, biosensing and UV sensing properties. Zhou *et al*. studied the UV sensing properties of SnO_2 nanowires, which were prepared by a laser-ablation chemical vapor deposition method [60]. Figure **7a** is a SEM image of the produced SnO_2 nanowires, which have smooth sidewalls and appear rather straight with diameter of about 20 nm and lengths on the order of 10 μm. The nanowires were fabricated into single nanowire field-effect transistors to check their electric transport behaviors and the corresponding gate-dependent I-V curves are shown in Fig. (**7b**). They showed linear behaviors indicating good Ohmic contacts. These nanowires show n-type semiconducting behaviors. Figure **7c** shows the current measured over time at constant V=50 mV and V_g=-10 V with UV light on and off six times. It was observed that the current increased dramatically and stabilized at a high-conductivity "on" state upon UV exposure. The current then landed at a low-conductivity "off" state after the UV light was off. Figure **7d** depicted two I-V curves taken with the device in the "on" and "off" states, respectively. The conductance of the device increased from 0.66 nS in dark to 760 nS upon UV illumination.

Aligned SnO_2 nanowire arrays were also configured as nanoscale photodetectors [57]. It was found that the conductance of the aligned nanowires increased from 0.12 μS in dark to 83.9 μS under UV light irradiation. Besides, in contrast to random network nanowires, the photocurrent of aligned nanowires showed strong polarization dependence, indicating a good alignment.

Similar to the improvement of gas sensitivity by decorating 1-D nanostructures with metallic nanoparticles, decorating metal oxide nanowires with metallic nanoparticles also provides a powerful way to enhance the UV sensing properties. For example, Chen *et al*. investigated the photocurrent enhancement of SnO_2 nanowires through Au nanoparticles decoration [58]. As shown in Fig. (**8**), the photocurrent increases with increasing light intensity from 2.5 V/m^2 to 774 W/m^2. Compared the curves in Fig. (**8**), it is very interesting to see that the photocurrent can be enhanced by up to about 110 %, when the nanowires are decorated with Au nanoparticles. The underlying mechanism for the enhancement is attributed to the formation of Schottky

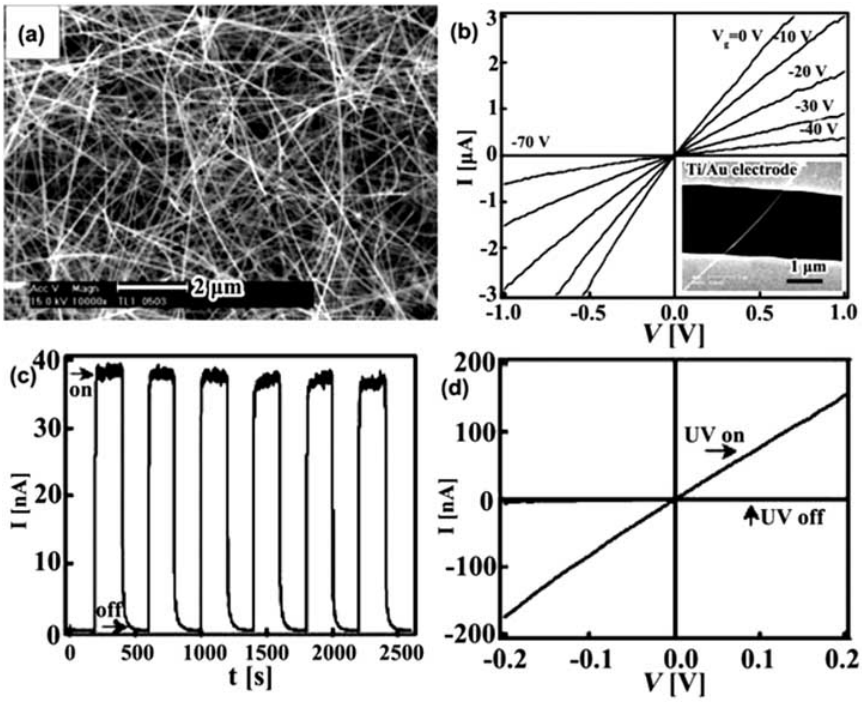

Fig. (7). (**a**) SEM image of laser-ablation synthesized SnO_2 nanowires. (**b**) gate-dependent I-V curves of a single SnO_2 nanowire device. (**c**) current vs time recorded with the UV illumination turned on and off repeatedly. (**d**) I-V curves taken before and after UV illumination. Reproduced with permission from *Adv. Mater*. **2003**, *15*, 1754. Copyright **2003** *Wiley-VCH*.

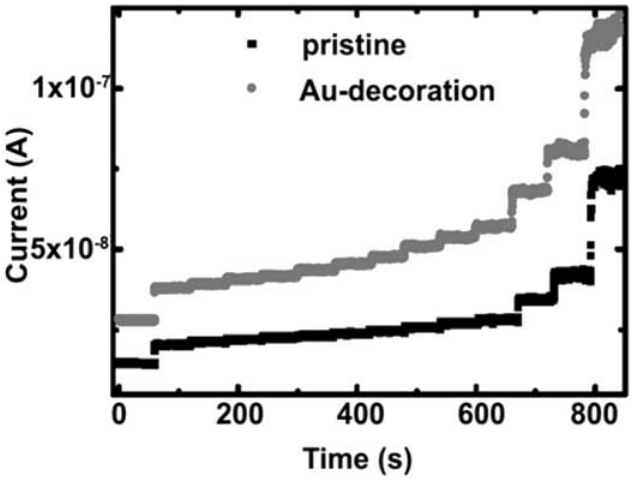

Fig. (8). Photoresponse of SnO_2 nanowires by UV illumination under excitation intensity. Reproduced with permission from *Opt. Exp*. **2008**, *16*, 16916. Copyright **2008** *OSA*.

junctions on the nanowire surface in the vicinity of metallic nanoparticles. They enhance the surface electric field and increase the spatial separation of photoexcited electrons and holes, which resulted in the prolonging of photoinduced electron life, and increasing the photocurrent gain. Similar results were reported by Pan *et al.* on Ag-decorated ZnO nanowires [51].

1-D ternary oxide nanostructures were also used to fabricate nanoscale photodetectors. Feng *et al.* synthesized single crystalline $ZnGa_2O_4$ nanowires via a low-pressure chemical vapor deposition method using Ga and ZnO as the sources [68]. The nanowires have diameters of several tens of nanometers and lengths of tens of micrometers. Figure (**9a**) and Fig. (**9a**) inset show the I-V curves of a single $ZnGa_2O_4$ nanowire device after and before UV illumination. Without UV illumination, the device has a current of 8.5 pA at a bias of 30 V. However, the current increase dramatically to 1 nA under UV illumination. Studies also found that the current of the device was sensitive to oxygen and temperature.

Ternary $ZnSnO_3$ nanowires were also fabricated into photodetectors [69]. Upon UV illumination, the current of a single device increased by about three orders of magnitude from 0.3 nA to 162 nA.

1-D III-V Group Nanostructures as Photodetectors

III-V group semiconductors are important materials that have many applications in electronics and optoelectronics. With a wide direct bandgap of 3.4 eV, GaN is an ideal candidate for ultraviolet applications. Zhou *et al.* synthesized GaN nanowires by thermal chemical vapor deposition method and then fabricated single nanowire field-effect transistors to investigate the photoconduction properties [72]. Figure (**10a**) depicted the I-V curves recorded from a single GaN nanowire FET before and after exposure to 254 and 365 nm UV light. Enhanced conduction was observed for the UV light irradiation of both wavelengths compared with the conduction without UV irradiation. The zero-bias conductance before and after UV light exposure is calculated to be 1.3 nS before exposure, 23.4 nS after 365 nm UV exposure, and 258.3 nS after 254 nm UV exposure, respectively. The enhanced conductivity was attributed to the photo-generated carriers in the nanowires.

Electrospun-grown GaN nanofibers were also used to fabricate high-performance photodetectors [73]. Studies found that the electrospun GaN nanofibers showed much higher sensitivity to UV detection than that of single crystalline GaN nanowires. The conductance of an electrospun GaN nanofiber increases by 830 times when UV was on. While a CVD-synthesized GaN nanowire only showed an increase of 78 to UV light. It is believed that the polycrystalline structure and rough surfaces resulted in much higher surface area-to-volume ratio, which led to more photogenerated carriers compared with a smooth GaN nanowire.

Lieber *et al.* fabricated polarization-sensitive photodetectors in which an individual InP nanowires serves as the device element, which were produced in a catalyst-assisted chemical vapor deposition process [76]. It was found that the conductance increased by two to three orders of magnitude

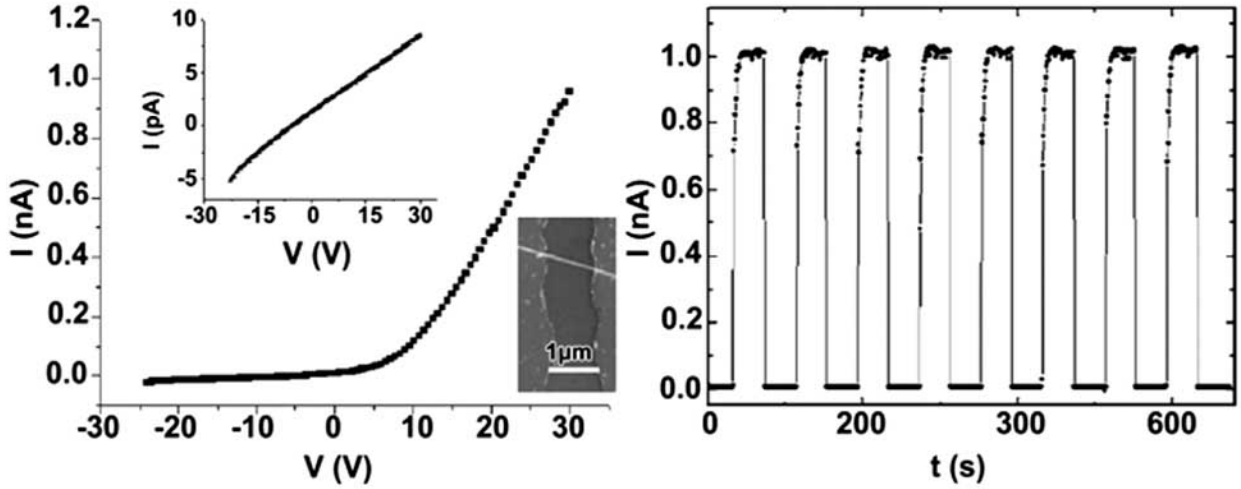

Fig. (9). (**a**) current vs voltage of $ZnGa_2O_4$ nanowire device under UV illumination. (**b**) real-time UV response of the $ZnGa_2O_4$ nanowire device. Reproduced with permission from *J. Appl. Phys*. **2007**, *102*, 074309. Copyright **2007** *American Institute of Physics*.

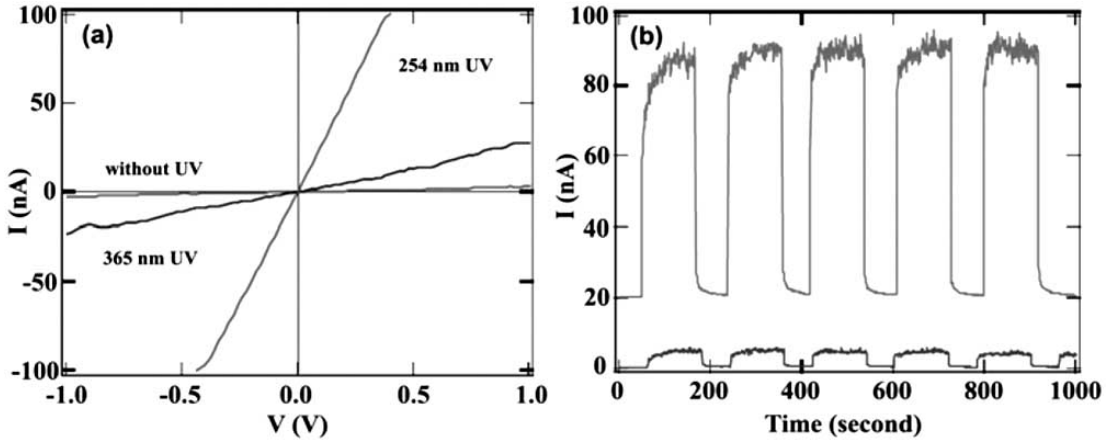

Fig. (10). (**a**) I-V curve of GaN nanowires before and after exposed to 254 nm and 365 nm UV light. (**b**) current vs time for the GaN nanowire with UV light repeatedly turned on and off. Reproduced with permission from *Chem. Phys. Lett.* **2004**, *389*, 176. Copyright **2004** *Elsevier B. V.*

with increasing excitation power density. The photoconductance also showed a striking polarization anisotropy with parallel excitation that is over an order of magnitude larger than the perpendicular excitation.

P-doped GaAs nanowires also showed very good photoconductance properties [75]. The nanowires were grown by molecular beam epitaxy technique. Studies found that the photocurrent was generated at the Schottky contacts between the nanowire and the metal source-drain electrodes.

1-D II-VI Group Nanostructures as Photodetectors

1-D II-VI group semiconducting nanostructures were also used for the fabrication of photodetectors because of their large variety of band gaps and a wide spectral response ranging from far-infrared to ultraviolet light. Lee *et al*. synthesized single-crystal CdS nanoribbons by a chemical vapor deposition method [80]. Figure **11** inset shows the optical microscopic image of the CdS nanoribbon device and a schematic diagram of the device configuration for photocurrent measurement. The I-V curves of a single CdS nanoribbon device exposed to UV lights with different wavelengths at a constant light intensity of 1.68 mW/cm^2 were shown in Fig. (**11**). The linear shape of the curves indicates good Ohmic contacts of the nanoribbon to the electrodes. The photoconductance at zero bias changed a lot under different UV irradiation. The calculated photoconductance is 0.793 nS for 500 nm UV irradiation, 128 nS for 490 nm UV irradiation compared with 0.021 nS in dark. Besides, the CdS nanoribbons showed changed photosensitivity in different atmosphere conditions through trapping electrons on the surface of the nanoribbons. Similar results were also reported by Wang *et al.* for the CdS nanobelts [78,79].

CdSe has a direct band gap of 1.75 eV at room temperature and a suitable to be configured as nanoscale photodetectors. Photoconductivity was also reported for CdSe single crystalline nanoribbons by Lee *et al*. as shown in Fig. (**12**) [82]. The inset is optical microscopy image of a single nanoribbon device and the schematic diagram of the photoconductive measurement. Figure **12a** showed the

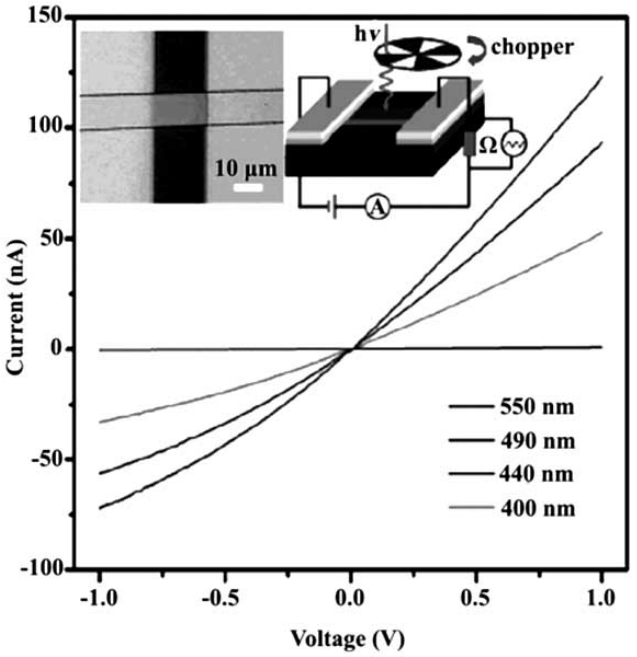

Fig. (11). I-V curves of a CdS single nanoribbon illuminated with light of different wavelength. Reproduced with permission from *Nano Lett.* **2006**, *6*, 1887. Copyright **2006** *American Chemical Society*.

wavelength-dependent I-V curves when the CdSe nanoribbon device was exposed to light at a constant intensity of 5.13 mW/cm^2, which revealed that the photoconductance was sensitive to the excitation wavelength. Furthermore, it was able to calculate the photoconductance under light irradiation with different wavelengths, which is 2816 nS at 760 nm, 1734 nS at 700 nm, 352 nS at 720 nm, 16.7 nS at 760 nm, 0.095 nS in a dark state, respectively. A cut-off wavelength of 710 nm was observed, indicating the photosensitivity of the CdSe nanoribbons is rather low for wavelengths longer than 710 nm. The response characteristics of the photoconductance of the CdSe nanoribbon detector to pulses of light irradiation switched at different frequencies

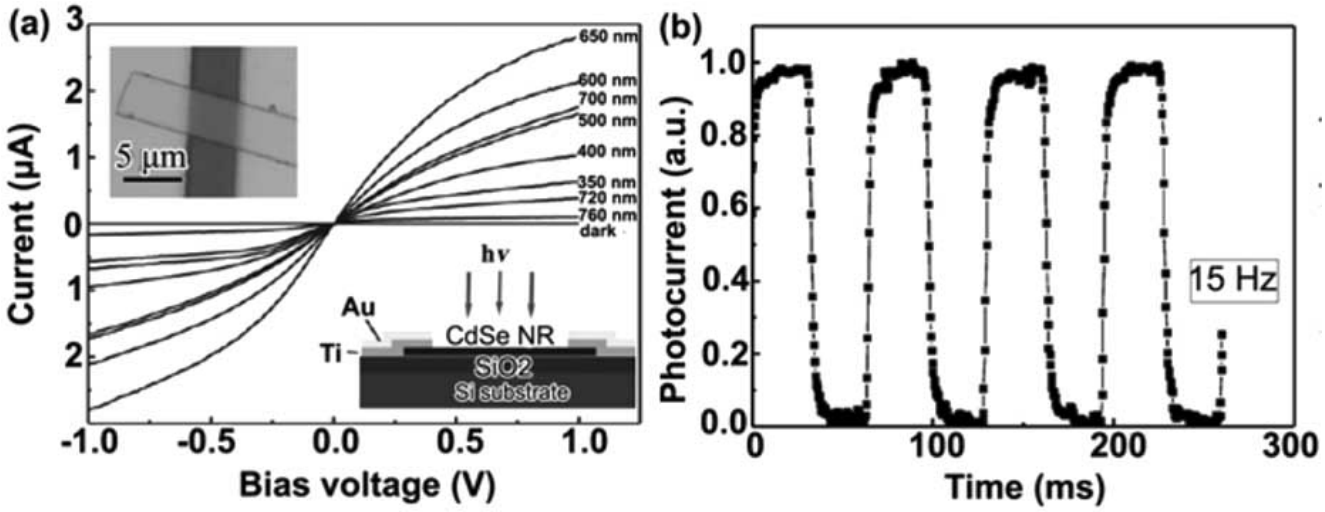

Fig. (12). (**a**) I-V curves of a CdSe individual nanoribbon illuminated with light of different wavelength at an intensity of 4.10 $mWcm^{-2}$. (**b**) response characteristics of the photoconductance of CdSe nanoribbon detector to light irradiation switched at a frequency of 15 Hz. Reproduced with permission from *Adv. Funct. Mater.* **2007**, *17*, 1795. Copyright **2007** *Wiley-VCH*.

were also studied. Figure **12b** shows the photocurrent vs time curves at a frequency of 15 Hz. High response speed was observed for the CdSe nanoribbon device.

Similar results were obtained by other researchers [81]. Besides 1-D CdS and CdSe nanostructures, other 1-D II-VI group semiconducting nanostructures were also found useful to be fabricated into photodetectors, such as ZnSe nanowires from solvothermal-annealing processes, ZnTe nanowires from hydrogen assisted thermal evaporation process [83,85].

Other 1-D Nanostructures as Photodetectors

Besides the above discussed 1-D metal oxide, III-V, II-VI group semiconducting nanostructures, 1-D nanostructures composed of other materials were also able to be fabricated into nanoscale photodetectors, as illustrated in Table **1**.

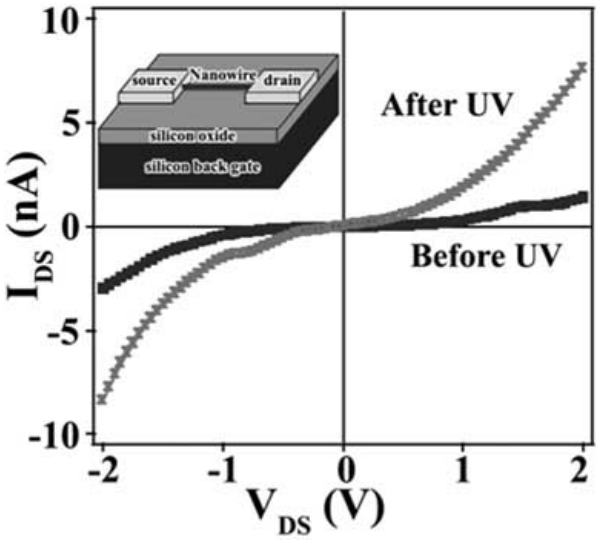

Fig. (13). I-V curves of the ZnS-decorated InP nanowire hetero-structures device before and after UV irradiation. Reproduced with permission from *Chem. Mater.* **2008**, *20*, 6779. Copyright **2008** *American Chemical Society*.

1-D hetero-nanostructures attracted great interests to be used as nanoscale photodetectors. Figure **13** shows the I-V curves of the ZnS-decorated InP nanowire heterostructures device before and after UV light with a wavelength of 254 nm irradiation [92]. The heterostructures, composed of single crystalline InP nanowires decorated with polycrystalline ZnS nanoparticles, were prepared via a simple thermal chemical vapor deposition method in which ZnS and InP powders were used as the source materials. The conductance showed enhancement after irradiation. The zero-bias conductance before and after the exposure was calculated to be 70 nS in dark and 813 nS after the exposure, respectively.

Lee *et al*. synthesized coaxial nanowires composed of a periodically twinned ZnSe single crystalline nanowire core and an amorphous silicon dioxide shell via a simple thermal evaporation process [91]. Figure **14a-d** depicted the TEM and HRTEM images of as-synthesized coaxial nanowires. All the nanowires have diameters of 50-150 nm and clean and smooth surfaces. Interestingly, it was found that all the nanowires showed periodic light/dark alternating contrast along the whole nanowires. Carefully studied by HRTEM revealed that the dark and light regions have a twinning relationship and share a common (11-1) plane. The angle between the two (111) planes is 141°. The photoconductance properties of the twinned coaxial $ZnSe/SiO_2$ nanowires were investigated and the corresponding I-V curves in dark and upon laser irradiation were shown in Fig. (**14e**). The conductance of the nanowires increased from 70.5 pS in dark to 123 pS after exposure. Time domain measurement was also performed and the result is shown in Fig. (**14f**). The current of the nanowire showed fast response to the variation of irradiation intensity.

Recently, many other kinds of 1-D nanostructures were also studied to investigate their possible applications in photodetectors, which include Si_3N_4 nanowires, InSe nanowires, coaxial InAsP/InAs nanowires, Se nanowires, p/i/n Si nanowires, Si nanowires, Ge nanowires, and RuO_2/TiO_2 core/shell nanowires [77,84,86,88,90,93].

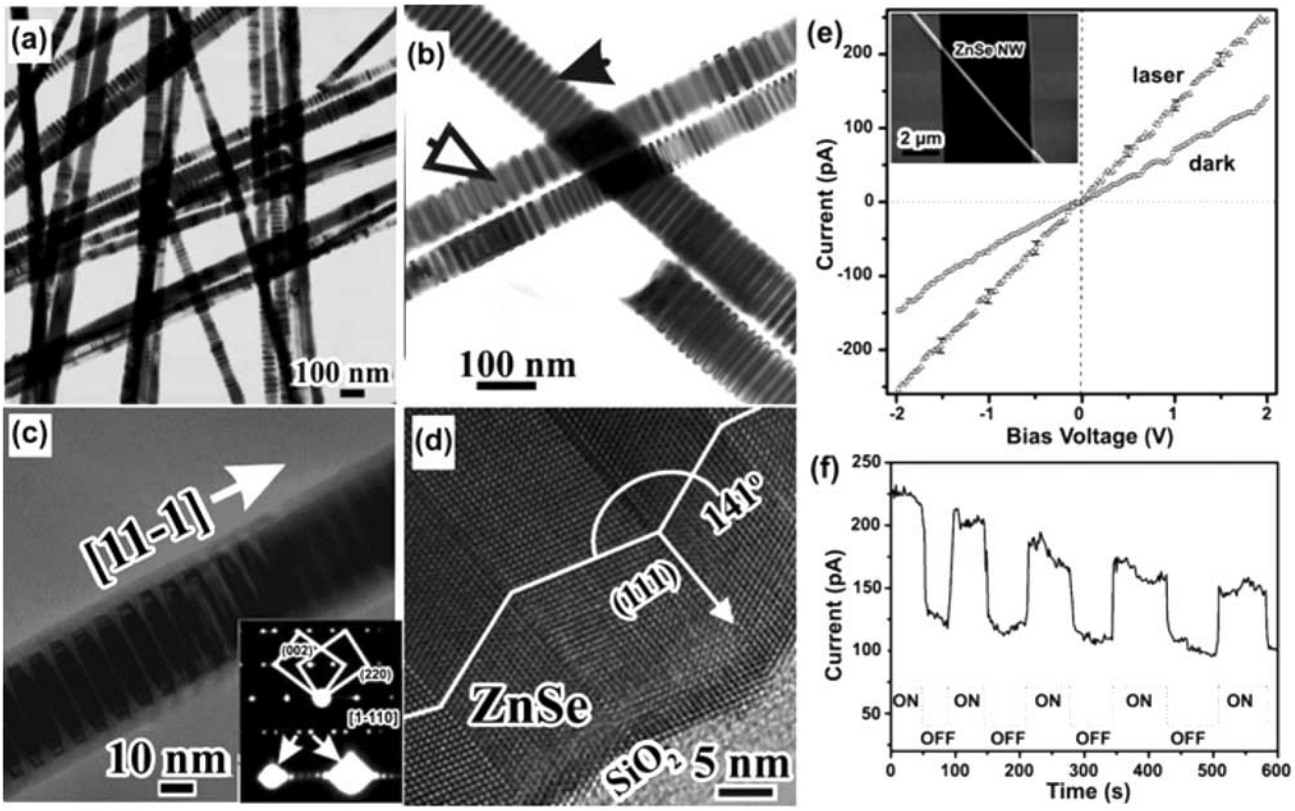

Fig. (14). (**a-d**) TEM and HRTEM images of the periodically twinned ZnSe/SiO_2 nanowires. (**e**) I-V curves of the single nanowire device in dark and under laser irradiation. (**f**) Time response of the nanowire device to a pulsed incidence laser. Reproduced with permission from *J. Phys. Chem. C.* **2009**, *113*, 834. Copyright **2009** *American Chemical Society*.

CURRENT & FUTURE DEVELOPMENTS

The state-of-the-art progress in 1-D nanostructure based photodetectors is reviewed in this paper. It is noted that photodetectors built on 1-D nanostructures have acquired fascinating achievements in the last decade. However, there are still a lot to be done to address the challenges that remain.

One important area is the assembly of 1-D nanostructures for real device applications. It is a hard but important work that needs intense research efforts. To improve the sensitivity of 1-D nanostructures based detectors, new materials synthesis techniques and device fabrication methods should be developed. It is believed that the sensitivity will be improved a lot with the produce of new structured 1-D nanomaterials. For example, complex 1-D heterostructures with special surface area, doping states and compositions will improve the device performance thus improve the photodetecting sensitivity. Considering the remarkable progress in 1-D nanostructures based photodetectors, many new discoveries should be expected further down the road.

ACKNOWLEDGEMENT

This work was supported by the High-level Talent Recruitment Foundation of Huazhong University of Science and Technology, the Basic Scientific Research Funds for Central Colleges (Q2009043), the Natural Science Foundation of Hubei Province (2009CDB326) and the Research Fund for the Doctoral Program of Higher Education (20090142120059).

CONFLICT OF INTEREST

The authors declare no conflict of interest.

REFERENCES

[1] Li Y, Qian F, Xiang J, Lieber CM. Nanowire electronic and optoelectronic devices. Mater Today 2006; 9: 18-27.

[2] Shen GZ, Bando Y, Ye C, Yuan X, Sekiguchi T, Golberg D. Single-crystalline nanotubes of II_3-V_2 semiconductors. Angew Chem Int Ed 2006; 45: 7568-7572.

[3] Shen GZ, Bando Y, Golberg D. Recent developments in single-crystal nanotubes synthesized from removable templates. Int J Nanotechnol 2007; 4: 730-749.

[4] Nagahara, L.A., Amlani, I.S.: US20077294560 (**2007**).

[5] Meerakker, V.D., Maria, J.E.A., Alfons, B., Kats, V., Maria, C.: US7357877 (**2008**).

[6] Kim, J.Y., Noh, C.H., Hwang, E.C.: US20067067237 (**2006**).

[7] Shen GZ, Cho JH, Yoo JK, Yi GC, Lee CJ. Synthesis of single-crystalline CdS microbelts using a modified thermal evaporation method and their photoluminescence. J Phys Chem B 2005; 109: 9294-9298.

[8] Shen GZ, Chen D. Self-coiling of $Ag_2V_4O_{11}$ nanobelts into perfect nanorings and microloops. J Am Chem Soc 2006; 128: 11762-11763.

[9] Patolsky F, Timko BP, Zheng G, Lieber CM. Nanowire-based nanoelectronic devices in the life science. MRS Bull 2007; 32: 142-149.

[10] Shen GZ, Bando Y, Chen D, Liu B, Zhi C, Golberg D. Morphology-controlled synthesis of ZnO nanostructures by a simple round-to-round metal vapor deposition route. J Phys Chem B 2006; 110: 3973-3978.

[11] Xia YN, Yang P, Sun Y, *et al.* One-dimensional nanostructures: synthesis, characteri-zation and applications. Adv Mater 2003; 15: 353-389.
[12] Shen GZ, Chen PC, Bando Y, Golberg D, Zhou C. Bicrystalline Zn_3P_2 and Cd_3P_2 nanobelts and their electronic transport properties. Chem Mater 2008; 20: 7319-7323.
[13] Shen GZ, Chen PC, Ryu K, Zhou C. Devices and chemical sensing applications of metal oxide nanowires. J Mater Chem 2009; 19: 828-839.
[14] Wang ZL. Splendid one-dimensional nanostructures of zinc oxide: a new nanomaterials family for nanotechnology. ACS Nano 2008; 2: 1987-1992.
[15] Yan R, Gargas D, Yang P. Nanowire photonics. Nat Photonics 2009; 3: 569-576.
[16] Martin CR. Nanomaterials: a membrane-based synthetic approach. Science 1994; 266: 1961-1966.
[17] Shen GZ, Bando Y, Golberg D. Self-assembled three-dimensional structures of single-crystalline ZnS submicrotubes formed by coalescence of ZnS nanowires. Appl Phys Lett 2006; 88: 123107.
[18] Kolmakov A, Moskovits M. Chemical sensing and catalysis by one-dimensional metal-oxide nanostructures. Annu Rev Mater Res 2004; 34: 151-180.
[19] Kong XY, Ding Y, Yang R, Wang ZL. Single-crystal nanorings formed by epitaxial self-coiling of polar-nanobelts. Science 2004; 303: 1348-1351.
[20] Shen GZ, Bando Y, Hu JQ, Golberg D. High-symmetry ZnS hepta- and tetrapods composed of assembled ZnS nanowire arrays. Appl Phys Lett 2007; 90: 123101.
[21] Pan Z, Dai Z, Wang ZL. Nanobelts of semiconducting oxides. Science 2001; 291: 1947-1949.
[22] Tian B, Kempa TJ, Lieber CM. Single nanowire photovoltaics. Chem Soc Rev 2009; 38: 16-24.
[23] Yu G, Cao A, Lieber CM. Large-area blown bubble films of aligned nanowires and carbon nanotubes. Nat Nanotechnol 2007; 2: 372-377.
[24] Patolsky F, Zheng G, Lieber CM. Nanowire sensors for medicine and the life sciences. Nanomedicine 2006; 1: 51-65.
[25] Shen GZ, Bando Y, Liu B, Tang C, Huang Q, Golberg D. Systematic investigation of the formation of 1D α-Si_3N_4 nanostructures by using a thermal-decomposition/nitridation process. Chem Eur J 2006; 12: 2987-2993.
[26] Shen GZ. Fabrication and characterization of metal oxide nanowire sensors. Recent Pat Nanotechnol 2008; 2: 160-168.
[27] Wang MCP, Gates BD. Directed assembly of nanowires. Mater Today 2009; 12: 34-43.
[28] Dong A, Tang R, Buhro WE. Solution-based growth and structural characterization of homo- and heterobranched semiconductor nanowires. J Am Chem Soc 2007; 129: 12254-12262.
[29] Shen GZ, Bando Y, Liu B, Golberg D, Lee CJ. Characterization and field-emission properties of vertically aligned ZnO nanonails and nanopencils fabricated by a modified thermal-evaporation process. Adv Funct Mater 2006; 16: 410-416.
[30] Lu W, Lieber CM. Nanoelectronics from the bottom up. Nat Mater 2007; 6: 841-850.
[31] Wang, Z.L., Summers, C.J., Wang, X., Graugnard, E.D., King, J.: US20087351607 (**2008**).
[32] Wang, Z.L., Kong, X.Y.: US20046863943 (**2004**).
[33] Wang, Z.L., Pan, Z.W., Dai, Z.R.: US20026586095 (**2002**).
[34] Zhou, C.W.: US20087394118 (**2008**).
[35] Wu, W., Corzine, S., Bratkovski, A.M., Wang, S.Y.: US20080310790 (**2008**).
[36] Yang, P., Kind, H., Yan, H., Law, M., Messer, B.: US20030121764 (**2003**).
[37] Pyun, J.C., Choi, H.J.: US20070131924 (**2007**).
[38] Fan Z, Ho JC, Jocobson ZA, *et al.* Wafer-scale assembly of highly ordered semiconductor nanowire arrays by contact printing. Nano Lett 2008; 8: 20-25.
[39] Baca AJ, Ahn JH, Sun Y, *et al.* Semiconductors wires and ribbons for high-performance flexible electronics. Angew Chem Int Ed 2008; 47: 5524-5542.
[40] Shen GZ, Chen D, Chen PC, Zhou C. Vapor-solid growth of one-dimensional layer-structured gallium sulfide nanostructures. ACS Nano 2009; 3: 1115-1120.
[41] Qian F, Li Y, Gradecak S, *et al.* Multi-quantum-well nanowire heterostructures for wavelength-controlled lasers. Nat Mater 2008; 7: 701-706.
[42] Hayden O, Agarwal R, Lu W. Semiconductor nanowire devices. Nano Today 2008; 3: 12-22.
[43] Prddes JD, Jimenez-Diaz R, Hernandez-Ramirez F, *et al*. Toward a systematic understanding of photodetectors based on individual metal oxide nanowires. J Phys Chem C 2008; 112: 14639-14644.
[44] Soci C, Zhang A, Xiang B, *et al.* ZnO nanowire UV photodetectors with high internal gain. Nano Lett 2007; 7: 1003-1009.
[45] Li Y, Valle FD, Simonnet M, Yamada I, Delaunay JJ. High-performance UV detector made of ultra-ling ZnO bridging nanowires. Nanotechnology 2009; 20: 045501 (1-5).
[46] Kind H, Yan H, Messer B, Law M, Yang P. Nanowire Ultraviolet photodetectors and optical switches. Adv Mater 2002; 14: 158-160.
[47] Hsueh TJ, Hsu CL, Chang SJ, *et al.* Crabwise ZnO nanowire UV photodetector prepared on ZnO:Ga/glass template. IEEE Trans Nanotechnol 2007; 6: 595-600.
[48] Lupan O, Chow L, Chai G, Chernyak L, Lopatiuk-Tirpak O, Heinrich H. Focused-ion-beam fabrication of ZnO nanorod-based UV photodetector using the in-situ lift-out technique. Phys Stat Sol A 2008; 11: 2673-2678.
[49] Kar JP, Das SN, Choi JH, Lee YA, Lee TY, Myoung JM. Fabrication of UV detectors based on ZnO nanowires using silicon microchannel. J Cryst Growth 2009; 311: 3305-3309.
[50] Suehiro J, Nakagawa N, Hidaka SI, *et al.* Dielectrophoretic fabrication and characterization of a ZnO nanowire-based UV detector. Nanotechnology 2006; 17: 2567-2573.
[51] Lin D, Wu H, Zhang W, Li H, Pan W. Enhanced UV photoresponse from heterostructured Ag-ZnO nanowires. Appl Phys Lett 2009; 94: 172103.
[52] Chen KJ, Hung FY, Chang SJ, Young SJ. Optoelectronic characteristics of UV photodetector based on ZnO nanowire thin films. J Alloy Compd 2009; 479: 674-677.
[53] Park D, Yong K. Photoconductivity of vertically aligned ZnO nanoneedle array. J Vac Sci Technol B 2008; 26: 1933-1936.
[54] Law JBK, Thong JTL. Simple fabrication of a ZnO nanowire photodetector with a fast photoresponse. Appl Phys Lett 2006; 88: 133114.
[55] Hsu CL, Chang SJ, Lin YR, *et al.* Ultraviolet photodetectors with low temperature synthesized vertical ZnO nanowires. Chem Phys Lett 2005; 416: 75-78.
[56] Lupan O, Chow L, Chai G. A single ZnO tetrapod-based sensor. Sens Actuators A 2009; 150: 184-187.
[57] Kim D, Kim YK, Park SC, *et al*. Photoconductance of aligned SnO_2 nanowire field effect transistors. Appl Phys Lett 2009; 95: 043107.
[58] Li CH, Chen TT, Chen YF. Photocurrent enhancement of SnO_2 nanowires through Au-nanoparticles decoration. Opt Exp 2008; 16: 1691616922.
[59] Wu JM, Kuo CH. Ultraviolet photodetectors made from SnO_2 nanowires. Thin Solid Films 2009; 517: 3870-3873.
[60] Liu Z, Zhang D, Han S, *et al.* Laser ablation synthesis and electron transport studies of tin oxide nanowires. Adv Mater 2003; 15: 1754-1757.
[61] Zhang D, Li C, Han S, *et al*. Ultraviolet photodetection properties of indium oxide nanowires Appl Phys A 2003; 77: 163-166.
[62] LiuX, Li C, Han S, Han J, Zhou C. Synthesis and characterization of CdO nanoneedles. Appl Phys Lett 2003; 82: 1950-1952.
[63] Feng P, Zhang JY, Li QH, Wang TH. Individual β-Ga_2O_3 nanowires as solar-blind photodetectors. Appl Phys Lett 2006; 88: 153107.
[64] Liao L, Yan B, Hao YF, *et al.* P-type electrical, photoconductive and anomalous ferromagnetic properties of Cu_2O nanowires. Appl Phys Lett 2009; 94: 113106.
[65] Fu XQ, Wang C, Feng P, Wang TH. Anomalous photoconductivity of CeO_2 nanowires in air. Appl Phys Lett 2007; 91: 073104.
[66] Hsu LC, Kuo YP, Li YY. On-chip fabrication of an individual α-Fe_2O_3 nanobridge and application of ultrawide wavelength visible-infrared photodetector/optical switching. Appl Phys Lett 2009; 94: 133108.
[67] Cheng L, Shao MW, Wang XH, Hu HB. Single-crystalline molybdenum trioxide nanoribbons: photocatalytic, photoconductive, and electrochemical properties. Chem Eur J 2009; 15: 2310-2316.
[68] Feng P, Zhang JY, Wan Q, Wang TH. Photocurrent characteristics of individual $ZnGa_2O_4$ nanowires. J Appl Phys 2007; 102: 074309.

[69] Xue XY, Guo TL, Lin ZX, Wang TH. Individual core-shell structured $ZnSnO_3$ nanowires as photoconductors. Mater Lett 2008; 62: 1356-1358.

[70] Wang SJ, Lu WJ, Cheng G, Cheng K, Jiang XH, Du ZL. Electronic transport property of single-crystalline hexagonal tungsten trioxide nanowires. Appl Phys Lett 2009; 94: 263106.

[71] Chen HY, Chen RS, Chang FC, Chen LC, Chen KH, Yang YJ. Size-dependent photoconductivity and dark conductivity of m-axial GaN nanowires with small critical diameter. Appl Phys Lett 2009; 95: 143123.

[72] Han S, Jin W, Zhang D, *et al.* Photoconduction studies on GaN nanowires transistors under UV and polarized UV illumination. Chem Phys Lett 2004; 389: 176-180.

[73] Wu H, Sun Y, Lin D, Zhang R, Zhang C, Pan W. GaN nanofibers based on electrospinning: facile synthesis, controlled assembly, precise doping, and application as high performance UV detectors. Adv Mater 2009; 21: 227-231.

[74] Lee JW, Moon KJ, Ham MH, Myoung JM. Dielectrophoretic assembly of GaN nanowires for UV sensor applications. Solid State Commun 2008; 148: 194-198.

[75] Thunich S, Prechtel L, Spirkoska D, Abstreiter G, Fontcuberta i Morral A, Holleitner AW. Photocurrent and photoconductance properties of a GaAs nanowire. Appl Phys Lett 2009; 95: 083111.

[76] Wang J, Gudiksen MS, Duan X, Cui Y, Lieber CM. Highly polarized photoluminescence and photodetection from single indium phosphide nanowires. Science 2001; 293: 1455-1457.

[77] Zhang JY, Chen YX, Guo TL, Lin ZX, Wang TH. Sub-band-gap photoconductivity of individual α-Si_3N_4 nanowires. Nanotechnology 2007; 18: 325603.

[78] Gao T, Li QH, Wang TH. CdS nanobelts as photoconductors. Appl Phys Lett 2005; 85: 173105.

[79] Li QH, Gao T, Wang TH. Optoelectronic characteristics of single CdS nanobelts. Appl Phys Lett 2005; 86: 193109.

[80] Jie JS, Zhang WJ, Jiang Y, Meng XM, Li YQ, Lee ST. Photoconductive characteristics of single-crystal CdS nanoribbons. Nano Lett 2006; 6: 1887-1892.

[81] Jie JS, Zhang WJ, Jiang Y, Lee ST. Single-crystal CdSe nanoribbon field-effect transistors and photoelectric applications. Appl Phys Lett 2006; 89: 133118.

[82] Jiang Y, Zhang WJ, Jie JS, Meng XM, Fan X, Lee ST. Photoresponse properties of CdSe single-nanoribbon photodetectors. Adv Funct Mater 2007; 17: 1795-1800.

[83] Meng QF, Jiang CB, Mao SX. Ohmic contacts and photoconductivity of individual ZnTe nanowires. Appl Phys Lett 2009; 94: 042111.

[84] Wang JJ, Cao FF, Jiang L, Guo YG, Hu WP, Wan LJ. High performance photodetectors of individual InSe single crystalline nanowire. J Am Chem Soc 2009; 131(43): 15602-3.

[85] Fang X, Xiong S, Zhai T, *et al.* High-performance blue/ultraviolet-light-sensitive ZnSe-nanobelt photodetectors. Adv Mater 2009; in press.

[86] Yang C. Barrelet CJ, Capasso F, Lieber CM. Single p-type/ intrinsic/n-type silicon nanowires as nanoscale avalanche photodetectors. Nano Lett 2006; 6: 2929-2934.

[87] Servati P, Colli A, Hofmann S, *et al.* Scalable silicon nanowire photodetectors. Phys E 2007; 38: 64-66.

[88] Liao ZM, Hou C, Zhao Q, Liu LP, Yu DP. Gate tunable photoconductivity of p-channel Se nanowire field effect transistors. Appl Phys Lett 2009; 95: 093104.

[89] Ahn YH, Park J. Efficient visible light detection using individual germanium nanowire field effect transistors. Appl Phys Lett 2007; 91: 162102.

[90] Chueh YL, Hsieh CH, Chang MT, *et al.* RuO_2 nanowires and RuO_2/TiO_2 core/shell nanowires: from synthesis to mechanical, optical, electrical and photoconductive properties. Adv Mater 2007; 19: 143-149.

[91] Fan X, Meng XM, Zhang XH, *et al.* Formation and photoelectric properties of periodically twinned $ZnSe/SiO_2$ nanocables. J Phys Chem C 2009; 113: 834-838.

[92] Shen GZ, Chen PC, Bando Y, Golberg D, Zhou C. Pearl-like ZnS-decorated InP nanowire heterostructures and their electric behaviors. Chem Mater 2008; 20: 6779-6783.

[93] Pettersson H, Tragardh J, Persson AI, Landin L, Hessman D, Samuelson L. Infrared photodetectors in heterostructured nanowires. Nano Lett 2006; 6: 229-232.

[94] Liu L, Peng Q, Li Y. Preparation of monodisperse Se colloid spheres and Se nanowires using Na_2SeSO_3 as precursor. Nano Res 2008; 1: 403-411.